Exciton and vibronic effects in the spectroscopy of bianthracene in supersonic beams

Lutfur R. Khundkar and Ahmed H. Zewail

Citation: The Journal of Chemical Physics **84**, 1302 (1986); doi: 10.1063/1.450521
View online: http://dx.doi.org/10.1063/1.450521
View Table of Contents: http://scitation.aip.org/content/aip/journal/jcp/84/3?ver=pdfcov
Published by the AIP Publishing

Exciton and vibronic effects in the spectroscopy of bianthracene in supersonic beams

Lutfur R. Khundkar and Ahmed H. Zewail[a)]
Arthur Amos Noyes Laboratory of Chemical Physics,[b)] California Institute of Technology, Pasadena, California 91125

(Received 1 October 1985; accepted 30 October 1985)

Excitation and dispersed fluorescence spectra of 9,9′-bianthracene in a supersonic expansion are reported. The spectra are anthracene-like, indicating that the rings are weakly coupled. Exciton effects are considered in the interpretation of the spectra. The torsional potential in S_1 is modeled as a double-well (Gaussian perturbation on a one-dimensional harmonic oscillator) with barriers to perpendicularity and planarity of ~ 30 and $\sim 1100\ \text{cm}^{-1}$, respectively. The S_0 torsional potential shows negative anharmonicity which is modeled as a quartic perturbation. Anthracenic modes in S_1 and S_0 are also assigned. Finally, measurements of S_1 fluorescence lifetimes up to $\sim 6000\ \text{cm}^{-1}$ excess energy in the excited state show no evidence of charge transfer.

I. INTRODUCTION

The anthracene molecule has been the focus of much work in this laboratory using crossed picosecond lasers and supersonic beams.[1] It has served as a model compound for the study of basic photophysical phenomena—nonradiative decays, intramolecular vibrational redistribution (IVR), and the effects of coherent excitation.[2] The characterization of these phenomena in substituted anthracenes is a natural extension and should help augment our understanding of them. In particular, the role of chain length of monosubstituted anthracenes in energy randomization has been addressed[3] and the manifestation of energy transfer in a bichromophoric molecule 9-[3-(4-*N*,*N* dimethylaniline)propyl] anthracene (ADMA) via the low frequency motions of the linker has also been detailed.[4]

Another candidate for study under isolated conditions is the "double molecule" 9-9′ bianthracene (BA). This molecule may be regarded as either a single molecule or as a covalently bonded dimer (end to end) of anthracene. Considered as an entity, BA provides an opportunity for the study of intramolecular torsional potentials and charge transfer. It is known from previous work on BA in solutions[5] and glasses[6] that the two anthryl moieties are perpendicular to each other in the ground state. In nonpolar solvents, its fluorescence is anthracene-like, implying that the two halves have little or no interaction. On the other hand, emission from BA in polar solvents is red shifted and structureless, and believed to result from relaxation to a charge transfer (CT) state.[7] The bathochromic fluorescence is inhibited in rigid polar glasses, demonstrating the strong correlation of torsional motion with electron transfer. A study of the torsional motion in the absence of intermolecular forces will be invaluable in identifying the role of the solvent in the charge transfer process and the effect of the torsion on IVR in anthracene.

In an exciton model, the two anthracene rings may be considered as nearest neighbors of a molecular crystal and BA may serve to illustrate excitation resonance interaction between the transition dipoles of the dimer, and between electronic and vibrational motions. The $S_1 \leftarrow S_0$ anthracene transition is aligned with the in-plane short axis. In BA, the two dipole moments corresponding to excitation of either anthracene ring are parallel and lie along the linking bond (see Fig. 1). The electronic coupling between the dipoles is invariant with respect to torsion about this bond and as a result, inferences about the potential energy surface may be drawn more readily from the spectra.

In this paper we present spectroscopic studies and picosecond lifetime measurements of bianthracene (9,9′-bianthryl) in supersonic jets. We have recorded the S_1 excitation spectrum from 374.4 to 345 nm and the dispersed fluorescence spectra of selected vibronic levels about the origin. These results allow us to characterize the low energy region of both the ground and excited state torsional potentials. Along this coordinate, S_0 appears flat bottomed and S_1 has a

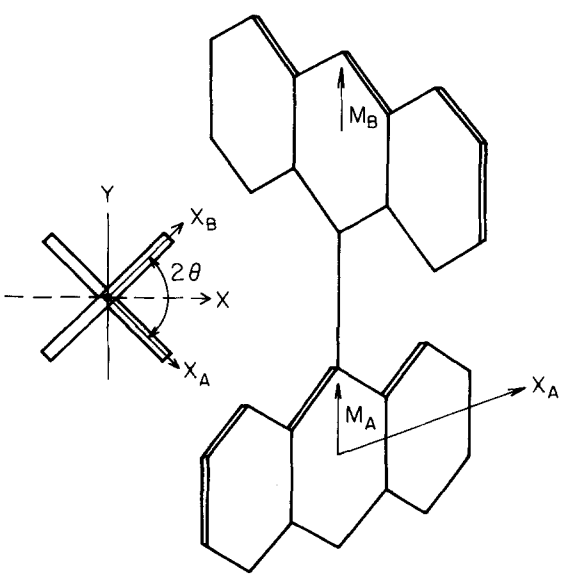

FIG. 1. Axis system and perspective of BA. The x and y axes bisect the dihedral angles between the planes defined by the anthracene rings. The z axis is coming out of the paper in the end-on view.

[a)] Camille and Henry Dreyfus Foundation Teacher–Scholar.
[b)] Contribution No. 7306.

 0021-9606/86/031302-10$02.10

well-defined double minimum. The measured fluorescence lifetimes as a function of the excess vibrational energy in S_1 and the model potential together indicate that there is no charge transfer in the isolated molecule at reasonable energies.

This article is organized in six subsections. After discussing the preliminary issues (symmetry, selection rules notation, and normal modes), we present the excitation spectrum and analyze the S_1 torsional mode. The assignment of other S_1 modes is followed by a similar analysis of the ground state. Finally, we discuss the relevance of the lifetimes measured to IVR and charge transfer.

II. EXPERIMENTAL

Excitation spectra were obtained from a pulsed jet apparatus[4] using a Nd^{+3}–YAG second-harmonic pumped tunable dye laser (5 ns pulses at 15 Hz) as the optical source. The dye-laser output was frequency doubled with a KDP crystal and the phase matching angle continuously optimized by a microprocessor controlled feedback system during a frequency scan. The sample was heated to ~190 °C to attain a vapor pressure that would give rise to an appreciable signal from the weaker transitions. Optimum cooling was obtained with 50 psi He (backing pressure) expanding through a 300 μ aperture. Ambient pressure in the expansion chamber was on the order of 10^{-4} Torr. The distance from the laser to the nozzle was maintained at 1.5 cm. The fluorescence signal was collected with $f/1$ optics, filtered through cutoff and bandpass filters, and detected with a photomultiplier tube (EMI 6256B). A second PMT was used to monitor the laser intensity. The fluorescence signal was normalized to the laser intensity using a dual channel boxcar averager (EG&G-PAR 162/164). The boxcar output was digitized by a voltage-to-frequency converter and stored on floppy disks.

Dispersed fluorescence spectra and S_1 lifetime measurements were done with a continuous-jet system.[2] Backing pressures of 40 psi He were used with a nominal 100 μ jet aperture. The chamber pressure was maintained at 10^{-3} Torr by a 12 in. bore ring-jet booster pump. The sample was heated to ~200 °C. The seeded beam was excited by the frequency-doubled output of an actively mode-locked Ar^+ pumped cavity dumped tunable dye laser. The laser to nozzle distance was maintained at 3 mm to ensure collision-free conditions in the region of interaction. Fluorescence was collected with a $f/1$ lens system and focused on the entrance slit of a microprocessor controlled $f/6.9$, 0.5 m monochromator. The dispersed fluorescence was detected beyond it with a fast photomultiplier. The signal was used for single-photon counting and the data recorded on a PDP 11/23 minicomputer. For measuring lifetimes, the slits were opened to their maximum width (3000 μ) and a 50 Å slice (typically centered at 3950 Å) of the total fluorescence profile was collected. The dispersed fluorescence spectra were recorded using narrowed slits (typically 100 μ or less).

The dye laser and monochromater wavelength scales were calibrated against known Ne lines observed in a Fe–Ne discharge lamp (see Ref. 4 for further details). The vibrational modes observed in the excitation spectra are reported to an accuracy of ~1 cm^{-1}. Assignments from the dispersed fluorescence spectra are reported to an accuracy of ~5 cm^{-1}. No vacuum corrections have been made. The relative intensities in the resolved fluorescence spectra have not been corrected for the spectral response of the PMT.

The fluorescence decay curves were fit to single exponentials and the quality of the fits were uniformly excellent as judged by the reduced χ^2 values.

BA was synthesized by the procedure described by many authors.[8] Briefly, 9-10 anthraquinone (Aldrich) was suspended in glacial acetic acid. A 2:1 mixture of tin and zinc dust (Matheson) by weight was added to the suspension, and the mixture heated under strong reflux while concentrated HCl was added dropwise. Once the reaction was complete, the mixture was cooled and the crystals separated by filtration. These were recrystallized first from toluene, and then from acetic anhydride. Recrystallization from pyridine gave a second compound which was not easily removed by subsequent recrystallization from other solvents. Further purification was achieved by repeated crystallization from chloroform. The melting point of the final product (pale yellow) was 312–313 °C (uncalibrated). The purity was corroborated by GC which indicated ⩾98% pure component. The mass spectrum showed a parent peak at 354 *m/e*. An elemental analysis was also consistent with a molecular formula $C_{28}H_{18}$.

III. RESULTS AND DISCUSSION

A. Preliminaries

1. Symmetries, selection rules, and notation

In the past we have employed the Pariser[9] axis system for anthracene[2] in which z is the anthracene out-of-plane axis, y is the short in-plane axis, and x is the long in-plane axis. The two anthracene halves of BA are mutually perpendicular in the ground electronic state, and the anthracene short axis is a unique C_2 rotation axis, conventionally designated z. The two other rotation axes for BA bisect the angle between the planes of each ring (Fig. 1). The correlation between the two molecular symmetry groups[10] must take into account local perturbations (site symmetry)[11] and is detailed in Table I. We shall use our previous notation for anthracene and D_{2d} symmetry representations for BA, with due attention to the different axis systems. In anthracene,

TABLE I. Correlation table for electronic states. D_{2h} (P) is for D_{2h} in Pariser notation where the short in-plane axis is the y axis. D_{2h} (M) is for D_{2h} in Mulliken notation where that axis is the z axis. In both C_{2v} and D_{2d}, the unique (z) rotation axis contains the 9,9′C–C bond.

D_{2h} (P)	D_{2h} (M)	→	C_{2v}	←	D_{2d}
A_g	A_g	→	A_1	←	A_1,B_2
B_{1g}	B_{3g}	→	B_2	←	E
B_{2g}	B_{1g}	→	A_2	←	A_2,B_1
B_{3g}	B_{2g}	→	B_1	←	E
A_u	A_u	→	A_2	←	A_2,B_1
B_{1u}	B_{3u}	→	B_1	←	E
B_{2u}	B_{1u}	→	A_1	←	A_1,B_2
B_{3u}	B_{2u}	→	B_2	←	E

TABLE II. Correlation table for the mixing of anthracene modes in BA. D_{2h}(P) and D_{2h}(M) have the same definitions as in Table I.

D_{2h}(P)	D_{2h}(M)		C_{2v}	D_{2d}	D_2
a_1	a_1	a_1	(in-phase)	a_1	a
b_{2u}	b_{1u}		(out-of-phase)	b_2	b_1
a_u	a_u	a_2	(in-phase)	b_1	a
b_{2g}	b_{1g}		(out-of-phase)	a_2	b_1
b_{3g}	b_{2g}	b_1	(in-phase)	e	b_2
b_{1u}	b_{3u}		(out-of-phase)	e	b_3
b_{1g}	b_{3g}	b_2	(in-phase)	e	b_3
b_{3u}	b_{2u}		(out-of-phase)	e	b_2

the transition dipole moment for $S_1 \leftarrow S_0$ lies along the y axis and corresponds to the ${}^1B_{2u}^+ \leftarrow {}^1A_g^-(\pi\pi^*)$ transition.[2,9] In BA, the ${}^1B_{2u}^+$ state for each anthryl moiety splits into B_2 and A_1 components (D_{2d}), the latter of which is optically disallowed from S_0 (*vide infra*).

Assuming that in its equilibrium geometry the two anthracenic halves of BA have the ${}^1A_g^-$ geometry of anthracene, the inertia tensor can be easily diagonalized. The algebra may be avoided by invoking symmetry arguments. In either D_2 or D_{2d} the three mutually perpendicular C_2 rotation axes are the three principle axes of the molecule (Fig. 1). For any dihedral angle 2θ the three principle moments of inertia[12] as functions of the twist angle are

$$(I_C)\quad I_x = 6.51\times10^{-40}(542 + 22.6\cos\theta + 471\cos^2\theta),$$

$$(I_B)\quad I_y = 6.51\times10^{-40}(542 + 22.6\sin\theta + 471\sin^2\theta),$$

$$(I_A)\quad I_z = 3.64\times10^{-37}\ \text{erg s}^2.$$

In the perpendicular configuration ($\theta = 45°$), BA is an accidental symmetric (prolate) top with rotational constants $A = 231$ and $B = C = 163$ MHz.

2. Anthracenic modes

We separate the treatment of normal modes into those derived from motions of the rings (*anthracenic*) and may therefore be correlated with anthracene normal modes and those resulting from the relative motion of the two ring systems. The two sets of anthracenic vibrations in BA will mix to form pairs of in-phase and out-of-phase vibrations. The symmetry representations may be derived from considerations of the corresponding motions in the site symmetry group (C_{2v}) and are listed in Table II. For instance, a_g vibrations (a_1 in C_{2v}) are split into a_1 and b_2 modes (D_{2d}). The amount of splitting depends on the interaction between the rings and may be different for each mode. Even for the anthracene a_g modes, this splitting may not be directly observable in electronic excitation since the b_2 component is optically inactive. We suggest that the splitting is relatively small on account of the very similar frequencies observed for these modes in BA and anthracene. Results in solution studies indicate that the two rings interact only weakly. A small splitting is also consistent with results for biphenyl[13] where the phenyl rings are planar.

Distortions from D_{2d} symmetry have been calculated[5,8] for BA in the excited state. The symmetry species of the anthracenic modes D_2 show that the in-phase combinations of anthracene a_u modes become allowed in this geometry, and we may expect weak bands corresponding to them in the spectra of BA.

TABLE III. The symmetry representations of the internal modes of BA in different point groups. For simplicity, we first describe the motions in D_{2h} (planar BA) and then correlate them to D_2 and D_{2d}.

	D_{2d}	D_{2h}(M)	D_{2h}(P)	D_2
C–C stretch	a_1	a_g	a_g	a
Torsion	b_1	a_u	a_u	a
Sym. bend[a]	e	b_{2u}	b_{3u}	b_2
Asym. bend[a]	e	b_{3g}	b_{1g}	b_3
Sym. rock[b]	e	b_{3u}	b_{1u}	b_3
Asym. rock[b]	e	b_{2g}	b_{3g}	b_2

[a] In-plane.
[b] Out-of-plane.

3. Internal modes

The 9,9′ C–C bond in BA gives rise to six vibrations that are unique to the molecule. The origin of these motions lies

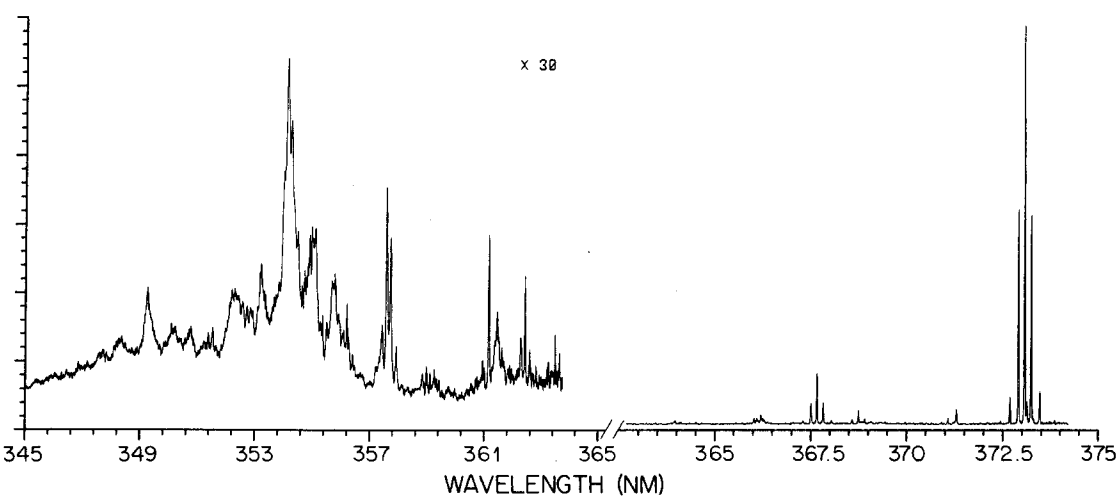

FIG. 2. The excitation spectrum of BA from 3744 to 3450 Å (see the text for details). Note the break in the energy axis and the change in the intensity scale. The sharp feature at 3610.7 Å is the origin transition of anthracene present as impurity.

in the degrees of freedom that are restricted by this bond. A description of their motion along with the symmetries for different BA geometries is presented in Table III. The a_1 C–C stretching mode is likely to have a frequency comparable to anthracene ring motions ($\gtrsim 1000\ cm^{-1}$) and may not be readily identified.

In the twisted geometry, the torsional mode transforms to a (D_2) and becomes symmetry allowed. To emphasize the nature of this mode which exhibits long progressions in all spectra, we label it τ.

The notation for the assignment of bands is the same as we have used for anthracene.[2] The labels $J_n^m K_{n'}^{m'}$... indicate transitions between combinations of vibronic modes $J,K,...$ with m,m'... quanta in the excited state and n,n'... quanta in the ground state. We do not assign labels to the modes of BA (except the torsion), but identify them with the corresponding anthracene mode where possible.

B. Spectroscopy of the excited state surface of BA

The excitation spectrum of BA (374.5–345 nm) is presented in Fig. 2 and the assignments of the bands are listed in Table IV. The 0_0^0 transition is assigned to the weak band at 3733.5 Å (26 785 cm^{-1}). This is in good agreement with the origin transitions of other mono-substituted anthracenes[3,4] (9-methyl- at 3710.2, 9-hexyl- at 3730.3 and ADMA at 3747.7 Å). The band positions are characteristic of anthracene, but the oscillator strength in this molecule appears to be mostly in the origin region.

1. Exciton states

The first order electronic interaction in BA may be described using the exciton model of molecular crystals.[11] With one resonant photon excitation to share between the two anthracene rings, the zero-order levels shift (site or solvent shift), and split (exciton or Davydov splitting) into states whose symmetries may be predicted from their representations in the site symmetry group. The exciton splitting of BA states corresponding to the $^1B_{2u}^+$ (D_{2h}) state of anthracene may be estimated using the point dipole model.[14] Since the two dipoles are parallel in this case, the interaction V is simply $V = -(2M^2/R^3)$, where M is the magnitude of the transition moment of the monomer, and R is the distance between the centers of charge. In this very simple (and perhaps naive) approximation, the dimer (BA) exciton splitting is $\sim 2200\ cm^{-1}$.[15] The two states correlate to a B_2 and an A_1 state, the latter being forbidden in one-photon optical transitions and higher in energy on account of the sign of the interaction. As only one of the exciton states is allowed, the excitation spectrum will be dominated by progressions in the torsional mode and BA modes corresponding to the in-phase combinations of the totally symmetric modes of anthracene in a single electronic manifold.

The origin of BA is 910 cm^{-1} to the red of the 0_0^0 transition in anthracene. This shift has three components: the effect of chemical substitution, the solvent shift, and the exciton splitting. The relative importance of these terms cannot be quantified in this study since we do not observe the A_1 exciton state. On this account, the comparison with the sub-

TABLE IV. Bands observed in the excitation spectrum of BA. The relative frequencies are in cm^{-1} and the reported intensities are normalized to the strongest transition.

Relative frequency	Relative intensity	Assignment	Anthracene modes
26 785	8.2	0_0^0	
15.5	52.4	τ_0^2	
24.3	5.5	He complex[a]	
27.8	100	τ_0^4	
39.5	53.9	τ_0^6	
55.8	6.8	τ_0^8	
74.0	0.8	τ_0^{10}	
98.7	0.3	τ_0^{12} ?[b]	
156.1	3.8		
171.7	1.4		
172.8	0.8		
184.2	0.4		
330.5	1.4	$315 + \tau_0^2$	
342.3	3.3	$315 + \tau_0^4$	
354.0	1.2	$315 + \tau_0^6$	
394.3	1.0	394	$385(12_0^1)$
410.2	5.5	$394 + \tau_0^2$	
422.2	12.5	$394 + \tau_0^4$	
433.8	5.3	$394 + \tau_0^6$	
449	0.8	$394 + \tau_0^8$	
524.3	1.1		
526.9	1.4	?	
529.8	2.5	?	
538.9	1.5	?	
543.6	1.4	?	
722.2	0.3		
734.3	0.4		$755(10_0^1)$?
752.5	0.3		
756.5	0.2		
786.2	0.2	$786 = 2\times 394$	$766(12_0^2)$
802	0.3	$786 + \tau_0^2$	
814.4	0.8	$786 + \tau_0^4$	
823.7	0.6		
825.6	0.4	$786 + \tau_0^6$	
855.6	0.2		
870.5	0.3		
873	0.3		
876	0.3	$860 + \tau_0^2$?	
883	0.4		
888	0.6	$860 + \tau_0^4$?	
927	0.3	?	
1 161	0.4	$1158 + 1147\tau_0^2$?	$1168(7/8_0^1)$
1 176	1.1	$1158\tau_0^2 + 1147\tau_0^4$	$1184(\overline{7}_0^1)$
1 187	1.6	$1158\tau_0^4 + 1147\tau_0^6$	
1 200	0.5	$1158\tau_0^6 + 1147\tau_0^8$	
1 280	0.3	1277?	
1 291	0.4		
1 296	0.7	$1277 + \tau_0^4$?	
		1300?	
1 319	0.6		
1 326	0.9	$1300 + \tau_0^4$?	
1 328	0.9		
1 336	0.9		
1 351	0.6	1352 + 1362?	
1 362	0.6		
1 381	1.3	$1360 + \tau_0^2$	$1380(6_0^1)$
1 391	1.4	$1360 + \tau_0^4$	
1 397	1.4	$1369 + \tau_0^4$	
1 430	1.3	$1430 + 1414\tau_0^2$?	$1420(5_0^1)$
1 448	2.1	$1430\tau_0^2 + 1414\tau_0^4$	$1420(5_0^1)$
1 450	2.0		
1 459	2.7	$1430 + \tau_0^4$	

TABLE IV. (*continued*)

Relative frequency	Relative intensity	Assignment	Anthracene modes
1 468	1.8	$1430 + \tau_0^6$	
...		1504	$1501(4_0^1)$
1 532	1.0	$1504 + \tau_0^4$	
1 605	0.8		
1 729	0.5	$1300 + 394\tau_0^4$?	
1 786	0.5	$1350 + 394\tau_0^4$?	
1 853	0.8	$1430 + 394\tau_0^4$	$1801(5_0^1 12_0^1)$

[a] We tentatively assign this band as a He complex (see the text).
[b] ? indicates the assignment is tentative. Spectral congestion and/or low intensities make a conclusive assignment impossible.

stituted anthracenes may be misleading. If we were to correlate the trend in bathochromicity with the size of the substituent, we would expect the origin of BA to lie between 3730 and 3748 Å.

2. Assignment of the torsional mode in S_1

The recorded excitation spectrum (26 680–26 800 cm^{-1}) shown in Fig. 3(a) shows a remarkable symmetry in the band spacings and intensity profile. This region was examined under different excitation conditions, varying pressure and carrier gases to exclude hot bands and complex bands. Using N_2, Ne, or Ar in the expansions, we have observed the presence of clusters at pressures large enough to guarantee satisfactory cooling. The optimum choice was He in agreement with results for ADMA.[4] The five most prominent bands appear in all recorded spectra and are assigned to excitation from a vibrationless BA molecule. We therefore assign the first weak band that can be positively identified with a "cold" transition as the 0_0^0 of BA (see later discussion).

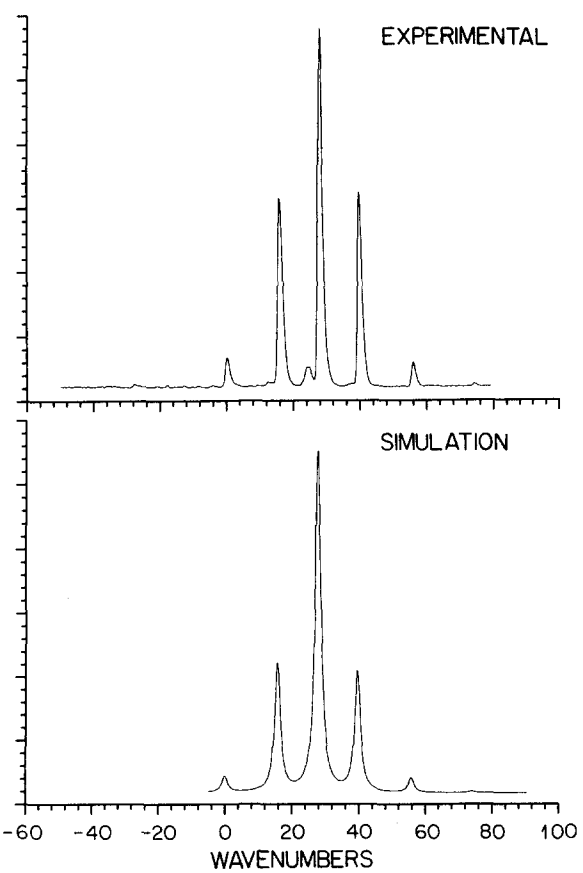

FIG. 3. A comparison between the observed excitation spectrum in the origin region and the spectrum predicted by the model potential. The top curve is the experimental spectrum. The simulated curve (bottom) assumes Lorentzian line shapes (FWHM ~ 1.0 cm^{-1}, chosen arbitrarily). The peaks are proportional to the calculated FC factors for transitions from the $v'' = 0$ level.

The most striking aspect of this spectrum is the symmetry in the band spacing and intensity profile. The difference in energy between consecutive bands exhibits a well-defined minimum as a function of vibrational energy. Such behavior is characteristic of linear-bent transitions[16] and implies the existence of a double minimum in the excited state potential energy surface. The height of the local maximum which separates the two minima generally corresponds to the smallest value of the energy difference between consecutive even (or odd) vibrational states.[16] With the assignment of the 0_0^0 as given above, this height must be ~ 30 cm^{-1}. It is important to note that the proper selection rule is $\Delta v = \pm 2n$ where n is zero or a positive integer. This is a consequence of the fact that the parity operator for reflection in the torsional coordinate about the ground-state equilibrium position is the parity operator for the excited state potential as well. Thus only wave functions having the same eigenvalue (i.e., $+1$ or -1) can have nonvanishing FC overlap.[17] With this in mind, the assignments of the observed bands are made as in Table IV.

The torsional Hamiltonian for BA may be written as[18,19]

$$H_T(\alpha) = -\frac{h^2}{4\pi^2 I_\alpha}\cdot\frac{\partial^2}{\partial\alpha^2} + \frac{V_2}{2}(1-\cos 2\alpha),$$

where α is the torsional angle and I_α is the moment of inertia of one anthryl moiety about the axis of rotation (C_z). For small amplitude oscillations or a high barrier (V_2), the potential term is approximately a harmonic oscillator. Adding a Gaussian perturbation onto this to represent a double-minimum potential,[20] we write the reduced Hamiltonian as

$$H_T(\xi) = -\left(\frac{V_2 h^2}{4\pi^2 I_\alpha}\right)^{1/2}\cdot\left[\frac{\partial^2}{\partial\xi^2} - (\xi^2 + Ae^{-B\xi^2})\right],$$

where

$$\xi = \left\{\frac{4\pi^2 V_2 I_\alpha}{h^2}\right\}^{1/4}\cdot\alpha$$

is the standard mass-weighted coordinate. The energy levels and wave functions of this Hamiltonian can be obtained numerically by first converting the differential operator into a tridiagonal band matrix and then finding its eigenvalues and eigenvectors.[21] The results of this numerical procedure were used to predict the band spacings. A linear least squares fit between the experimental intervals and these predictions yields a slope which is the fundamental frequency and a statistic χ^2, the sum of deviations squared. A and B were varied independently to generate a local map of the distribution of $\chi^2(A,B)$. A contour map of this distribution was used to choose a pair of values (A^*,B^*) that minimized χ^2. The exci-

TABLE V. A comparison of observed and predicted excitation bands near the origin. The calculated bands considers transitions involving up to three quanta in the ground state torsional mode only.

Observed bands (cm^{-1})	Predicted transitions (cm^{-1})	Assignment
− 29.0	− 29.1	τ_2^0
− 23.4		...
− 20.2		...
− 18.2		...
− 13.9	− 14.2	τ_1^1
− 4.7		
0.0	0.0	$\tau_0^{0\,a}$
2.0	2.0	τ_1^3
11.0	10.6	τ_2^6
15.5	15.8	$\tau_0^{2\,a}$
	17.1	τ_1^5
24.3		He complex[b]
	26.7	τ_2^8
27.8	27.9	$\tau_0^{4\,a}$
32.8	33.0	τ_1^7
39.5	39.7	$\tau_0^{6\,a}$
45.9	45	τ_2^{10}
50.3	50.5	τ_1^9
55.8	55.8	$\tau_0^{8\,a}$
74.0	74.1	τ_0^{10}

[a] These values were used to choose the S_1 potential.
[b] See Table IV.

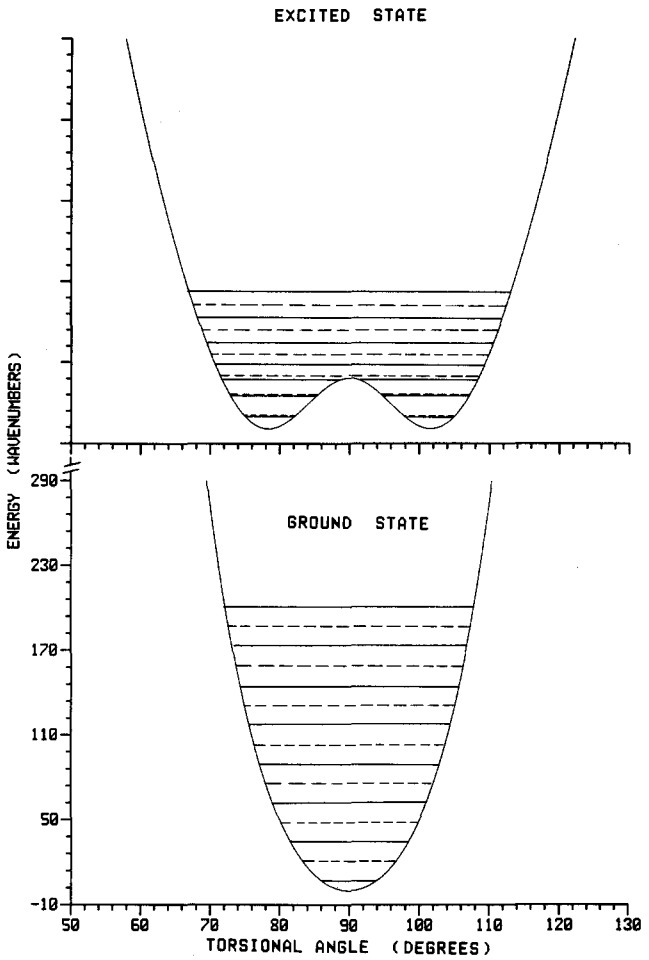

FIG. 4. The model potentials for the excited and ground state of BA. The upper double well represents the excited state. The lower one is a harmonic potential plus a quartic perturbation and is used to describe the ground state. The solid and dashed lines show levels of even and odd quanta, respectively.

tation bands predicted using this best-fit potential are compared to the experimental results in Table V. The potential is shown in Fig. 4. Assuming the ground-state potential described below, we obtain FC factors for the torsional progression in S_1 by numerical integration of the product of the generated wave functions. The excellent agreement between predicted and observed intensities (Fig. 3) for these bands lends strong support to the assignment of this progression.

The potential parameters allow one to calculate the S_1 equilibrium torsional angle as 78°, and the small barrier to perpendicularity as 38 cm^{-1}.[22] The fundamental frequency of 12.3 cm^{-1} corresponds to a barrier to planarity of 1100 cm^{-1} in the excited state. This barrier to planarity is lower than what may be intuitive. Severe repulsive forces will be encountered in forcing the 1,8 and 1′,8′ H atoms into the same region of space. The core repulsion will be accommodated by distortions of the molecular framework which may account for such a low value.

The observation of a small barrier at $\alpha = 90°$ is consistent with PPP[5] and force-field calculations.[7] Our value for the equilibrium torsional displacement is in excellent agreement with their calculated values of 78° and ~70°, respectively. The origin of this barrier may be traced to configuration interaction between the exciton states and the energetically higher charge-resonance states. In more physical terms, the barrier to perpendicularity is a manifestation of the balance between charge-resonance (CR) interactions and nonbonded repulsions. As the two parts twist toward a planar geometry, the overlap of π orbitals increases and the CR increases, leading to a lowering of the electronic energy. The same motion brings the four H atoms closer together and the steric repulsion destabilizes the state.

The common model for a torsional potential is a truncated sum of cosines with periodicities dictated by the symmetry of the problem. The double-well potential may also be modeled as[18,23]

$$V_{\text{torsion}} = \sum_{N=2,4} V_N(1 - \cos N\theta).$$

Other approaches to this problem in the context of inversion or quasilinear transitions have used Gaussian barriers or higher order polynomials. We have chosen to use a Gaussian perturbation because this allows us to vary the curvature of the potential in the region of interest (i.e., where the observed bands are) without increasing the number of parameters in the fit.

Another more insidious problem involves the assignment of the 0_0^0 transition. Suppose the assigned transition is in reality the τ_0^{2n} one (the others will be τ_0^{2m+2n}, etc.). The trend in the intensity distribution indicates that the τ_0^{2n-2} band may be too weak to be observed. There are a few weak transitions to the red of 3733.5 Å, but none can be clearly identified as being derived from the vibrationless level in S_0. Under slightly warmer excitation conditions, this region of

the spectrum is swamped by transitions from vibrationally excited BA, but the possibility of there being other cold transitions obscured by these bands cannot be ruled out. We have also carried out similar calculations assuming that the first line in our spectrum was the τ_0^4 transition. The potential obtained in this case reproduces the excitation spectrum equally well. The barrier at 90° is 76 cm^{-1}, and the equilibrium torsional angle is 75°. The new fundamental frequency is 14.3 cm^{-1}, corresponding to a barrier to planarity of 1400 cm^{-1}.

Yamasaki *et al.* have very recently communicated their preliminary results from a similar spectroscopic study of BA.[24] A comparison of our spectra with theirs shows our expansion conditions afford significantly better vibrational cooling; many of the weak features in their spectra are due to hot bands. The differences between the model potentials can be explained by the choice of the true 0_0^0 transition. Yamasaki *et al.* estimate a value of 26 686 cm^{-1} and we assign an experimentally observed band as the origin, with some qualification. The intensity profile about the origin suggests that the direct observation of the S_1 origin will be next to impossible if 26 686 cm^{-1} is the true 0_0^0.

3. Assignment of other S_1 modes

We attempt to assign observed bands in the excitation spectrum by comparison with published spectra of anthracenes.[2,3] Figure 2 shows very few bands with significant intensity. The two sets of bands at 315 and 394 cm^{-1} show intensity and interval patterns identical to the origin region. The assignment of these bands are therefore readily made. The first overtone of the 394 cm^{-1} fundamental is observed at 786 cm^{-1} and the relative intensities follow a regular FC pattern.

Above 1100 cm^{-1} the spectrum shows evidence of congestion. None of the discernible bands exhibit the 0–0 pattern, but appear to be two or more such patterns overlapped. Assuming that the vibrational substructure of these bands do in fact follow the intensity distribution seen near the origin, the peak of each of them should be assigned as a combination of some transition and τ_0^4. Using this argument, we identify most of the fundamentals in BA that correspond to a_g fundamentals in anthracene S_1.

4. Comparison with other systems

The free-jet spectroscopy of a similar bonded dimer 1,1′binaphthyl (BN) has been reported by Jonkman and Wiersma.[25] The S_1 (^1L_b) state in naphthalene is long axis polarized. The site symmetry group of the dimer C_2 and both exciton states are observed. In BN, torsion about the 1,1′ bond results in a change in the excitation exchange interaction, which has been measured as ~ 60 cm^{-1}. Vibronic mixing between S_1 and the more strongly allowed S_2 (^1L_a) states is thought to induce intensity in the exciton states.

The spectroscopy of BA is simpler. The exciton interaction is independent of torsion and there are no low-lying states with large oscillator strength to participate in vibronic mixing.[5] We cannot identify the origin of the forbidden exciton state, but we are able to assign the anthracene-like spectra assuming only one optically active exciton state.

Low frequency fundamentals showing long progressions in optical transitions have been observed in the spectra of aryl substituted aromatics such as ADMA,[4] BN[25], biphenyl,[26] and 9-phenylanthracene.[23] In all cases except the first, the progression has been attributed to transitions between single-well and double-minimum potentials along the torsional coordinate in different surfaces. This is quite similar to the analysis presented here.

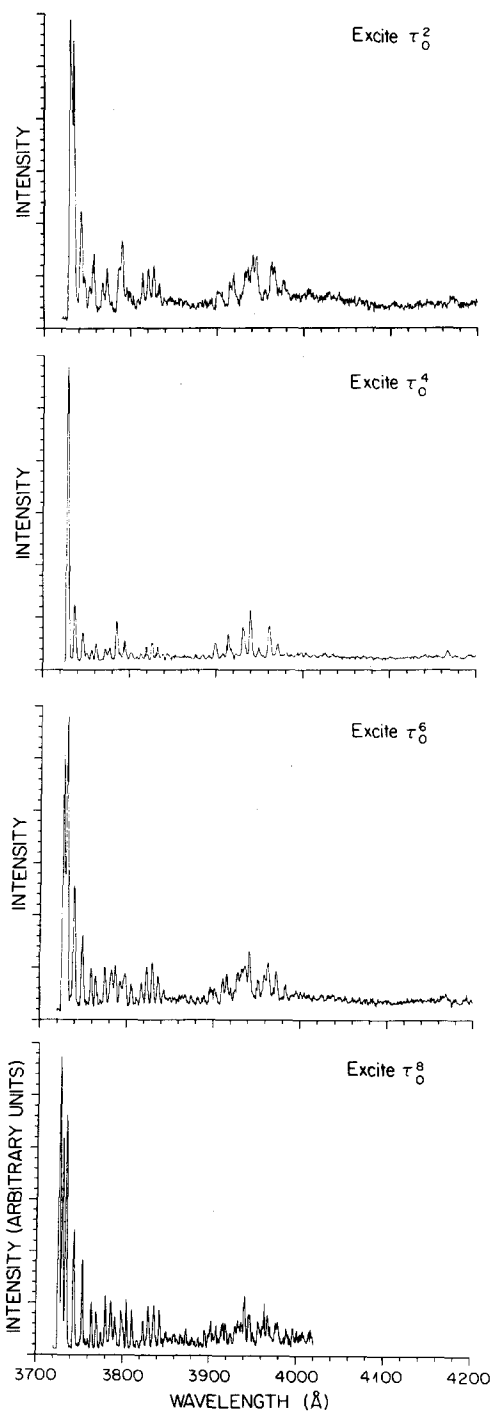

FIG. 5. Fluorescence spectra obtained after excitation to different bands of the torsional progression. The monochromator resolution was ~ 10 cm^{-1}. The alternating intensity is due to changing FC factors.

C. Spectroscopy of the ground state surface

The dispersed fluorescence spectra obtained on excitation to the various bands in the origin region are shown in Fig. 5 and bands with significant intensity are listed in Table VI with their tentative assignments. Prominent features in these spectra are (1) a long progression in the torsional mode, (2) bands closely corresponding to anthracene S_0 vibrations observed in 0_0^0 fluorescence in anthracene, and (3) progressions of combinations of the torsional mode with the anthracenic fundamentals.

1. Assignment of the S_0 torsional mode

The progression of bands in the fluorescence spectrum shows negative anharmonicity, implying that the S_0 potential is flat-bottomed with steep sides. This is consistent with calculated potentials. Symmetry arguments preclude all odd powers of ξ in the potential. In a first approximation, the problem may be treated as a quartic perturbation on a harmonic oscillator. The first order correction to the energies gives us an expression[27]

$$E_n = h\nu(n+\tfrac{1}{2}) + \tfrac{3}{2}\beta\left(\frac{h}{m\nu}\right)^2 \cdot (n^2+n+1)$$

for the energy identified with the quantum number of the unperturbed problem. A Birge–Spöner fit gives a value of 0.21 cm^{-1} for the anharmonic correction and 13.5 cm^{-1} for the fundamental frequency. The potential energy as a function of the twist angle is shown in Fig. 4. The assignment of the torsional progression is based on the $\Delta v = \pm 2n$ selection rule described earlier.

We have calculated FC factors for each of the fluorescence spectra shown in Fig. 5 using the S_1 wave functions obtained previously. The intensity distributions are predicted quite well, especially below 100 cm^{-1}. As a consistency check for our model, we have simulated excitation spectra for different temperatures. Comparison with spectra obtained under warm expansions (Fig. 6 and Table V) shows that our model can explain these adequately.

TABLE VI. Assignment of the dispersed fluorescence spectra of various torsional levels in S_1. The intensities are normalized to the strongest tradition in each spectrum.

Relative energy	Relative intensities τ^2	τ^4	τ^6	τ^8	Assignment	Anthracene
0	100	100	87	100	τ_0	
29	93		100	74	τ_2	
61		20		81	τ_4	
90	38		44		τ_6	
122		10		44	τ_8	
157	14	3	28		τ_{10}	
195	24	4		33		
231		7	17	7	?	232?
272	15		14	20		
305	20	5	7	16		
345	9	5	17	10		
400		14	16		$(400)_1^0 + \tau_0$	$390(12_1^0)$
428	28		18	20	$(400)_1^0 + \tau_2$	
463		7	12	15	$(400)_1^0 + \tau_4$	
505			15	17		
552			12	21		
594	18	3	7	18		
636	20	5	12	7		$624(11_1^0)$?
682	20	7	18	13		
725	15	5	19	18		
770	10		14	19		$753(10_1^0)$?
810	10		10	17		
863		3	7	10		
1172		14	11		$(1170)_1^0 + \tau_0$	$1165(8_1^0)$
1210			10	13	$(1170)_1^0 + \tau_2$	
1265	15	16	14		$(1265)_1^0 + \tau_0$	$1263(7_1^0)$
1294	18		15		$(1265)_1^0 + \tau_2$	
1378	19	12	16		$(1378)_1^0 + \tau_0$	$1403(6_1^0)$
1411			17	13	$(1378)_1^0 + \tau_2$	
1435	24	18	18	13	$(1435)_1^0 + \tau_0$	$1486(5_1^0)$
1461	23		23	22	$(1435)_1^0 + \tau_2$	
1495		5		16	$(1435)_1^0 + \tau_4$	
1574	21	12	15		$(1574)_1^0 + \tau_0$	$1566(4_1^0)$
1603	20		19	19	$(1574)_1^0 + \tau_2$	
1631		6		15	$(1574)_1^0 + \tau_6$	
1661	15		16		$(1574)_1^0 + \tau_4$	

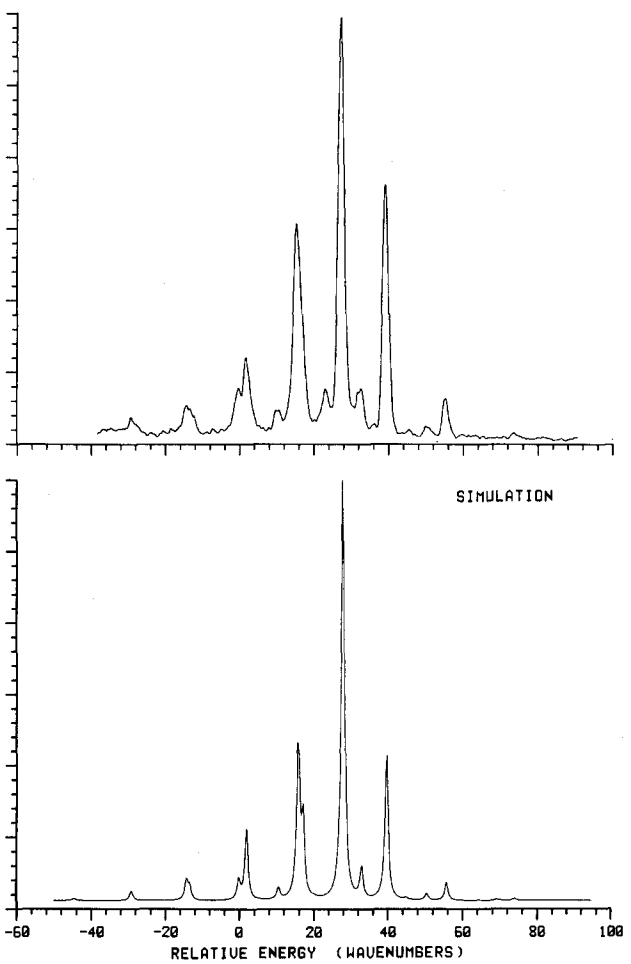

FIG. 6. Experimental vs simulated excitation spectra in warm expansions. A vibrational temperature of 12 K was assumed for the simulation. The experimental spectrum was obtained with He as carrier gas and 10 psi backing pressure. The weak band at 24 cm^{-1} above the assigned 0_0^0 is not present in the simulations. This feature is pressure dependent and has been assigned as a complex band.

5. Assignment of other S_0 modes

Since the τ_0^4 is the strongest line in the excitation spectrum, we expect it to show fluorescence very similar to a typically 0^0 spectrum. In particular, $n = 0$ will have the largest overlap for transitions from τ^4 to combinations of the type $a_m\tau_n$ (a is any normal mode) and the torsional progression will be the shortest. We have used this criteria and the known values of S_0 monomer vibrations[2] to assign BA fundamentals. Subsequently, the assignments of the other spectra were made by assuming that the combinations observed involve the same τ_n as seen in the progression of the pure torsion.

The 400, 1170, 1265, and 1574 cm^{-1} modes are assigned with confidence. The bands at 1378 and 1435 cm^{-1} are assigned by correspondence with S_1 modes. The differences in frequencies of these modes in S_1 and S_0 are smaller than in anthracene.The mode corresponding to ν_{10} in anthracene appears to be strongly mixed with the higher torsional quanta of ν_{12}. This is indicated by the change in the torsional band spacings from $\sim 30\ cm^{-1}$ near the origin to $\sim 45\ cm^{-1}$ in the set (594, 636, 682, 725, 770, and 810). The intensity profile across this set changes in a regular manner as the quantum number of the initially excited state changes from 2 through 8.

D. SVL fluorescence lifetimes, IVR, and charge transfer

The fluorescence decay rates following single vibronic level (SVL) excitation in BA have been recorded and the data plotted in Fig. 7. Two basic types of behavior have been identified. At low energy, the rates increase with energy, although this dependence is irregular for certain modes, particularly within the low frequency progression about the 0_0^0. At higher energies, the rates become nearly constant with vibrational energy (saturation effect) and do not exhibit mode selectivity. The saturation lifetime is about 7 ns and occurs at a threshold energy of about 300 cm^{-1}.

In an earlier paper,[3] we investigated this saturation behavior in a series of anthracene derivatives, arriving at the following set of data for the saturation lifetime and threshold energy; anthracene (6 ns, 1800 cm^{-1}), 9-methylanthracene (9 ns, 1000 cm^{-1}), 9-hexylanthracene (10 ns, 400 cm^{-1}) and ADMA (10 ns, 400 cm^{-1}). The saturation effect in the fluorescence lifetimes is indicative of a nonradiative decay channel with a small electronic energy gap.[2,28] In anthracene and its derivatives, this presumably involves intersystem crossing (ISC) from S_1 to near lying triplet levels.[2] As discussed elsewhere, the threshold energy for rate saturation correlates with increased IVR.

Charge transfer in an isolated molecule is manifested by broadened, red-shifted fluorescence and can be monitored by time-resolved measurements of resonance or CT fluorescence. The formation of a stable charge-transfer complex will be observable as a new channel for nonradiative decay.[4] The rates vs excess energy show no evidence of such a channel up to $\sim 6000\ cm^{-1}$ in S_1. This indicates that CT is induced by solvent interactions as suggested by Rettig and Zander.[7] This is not surprising since direct orbital overlap is small in BA and the symmetry of the molecule dictates that the driving force is small.

IV. CONCLUSIONS

Our beam results and analysis show that the S_1 torsional potential has a barrier to perpendicularity of $\sim 38\ cm^{-1}$. The torsional frequency is 12.3 cm^{-1} and the equilibrium torsional angle is 78°. This is a minimum value of the twist from the perpendicular geometry. With a different choice of the assignment of the 0_0^0, the barrier at $\theta = 90°$ and the fundamental frequency will increase and the equilibrium geometry will deviate more from the perpendicular. The ground

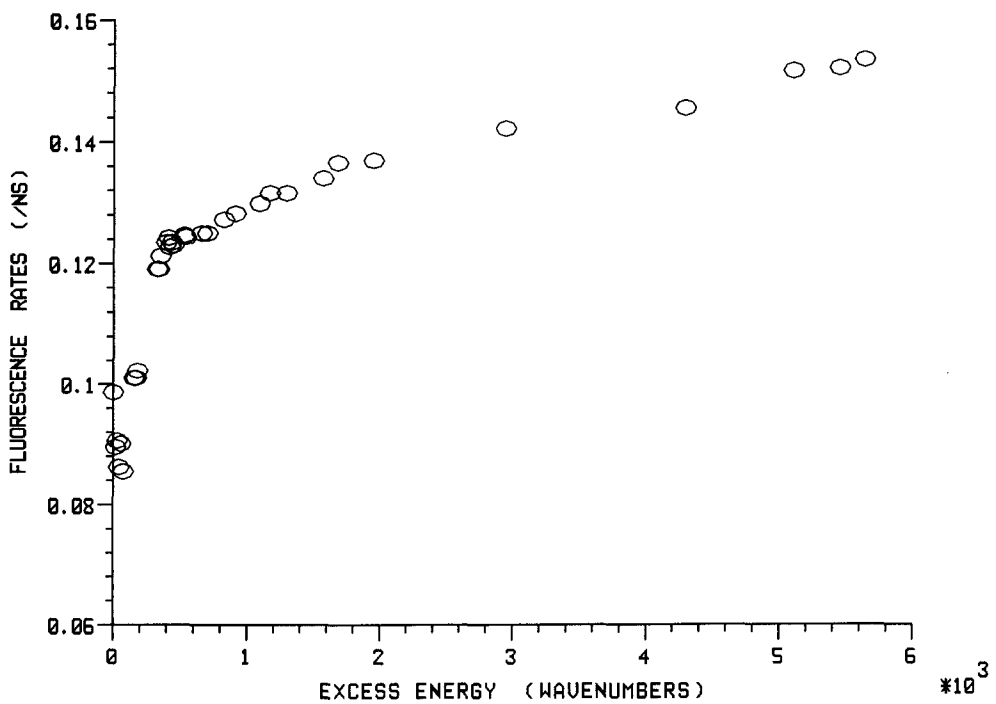

FIG. 7. Fluorescence rates as a function of excess energy in S_1. The saturation effect resembles the trend in anthracene and substituted anthracenes. The lack of any new channels of rapid nonradiative decay is evidence against CT occurring in the isolated molecule.

state potential along this coordinate has a flattened bottom and exhibits negative anharmonicity (0.21 cm^{-1}) but no barrier at 90°. Thus the ground state equilibrium geometry is perpendicular. The torsional frequency is 13.5 cm^{-1}, corresponding to a barrier to planarity of ~ 1500 cm^{-1}.

We have identified most of the a_g modes of anthracene in the S_0 and S_1 manifolds of BA. There is a close resemblance of the results shown here to anthracene excitation and fluorescence spectra and this behavior is indicative of small interaction between the two anthracene rings. Experimental results from similar studies in nonpolar environments have indicated the same conclusion.

No charge transfer fluorescence emission is observed in the isolated molecule independent of the excess energy in S_1, unlike the results in ADMA. This is taken to verify that charge transfer can occur only with solvent stabilization.

ACKNOWLEDGMENTS

It is a pleasure to acknowledge the National Science Foundation (Grant No. DMR-8521191) for its support of this research. We also thank Dr. Jack A. Syage and Dr. Peter M. Felker for their generous assistance in recording the spectra and for many helpful discussions.

[1]A. H. Zewail, Discuss. Faraday Soc. **75**, 315 (1983).
[2]W. R. Lambert, P. M. Felker, and A. H. Zewail, J. Chem. Phys. **81**, 2195, 2209, 2217 (1984); P. M. Felker and A. H. Zewail, *ibid.* **82**, 2961, 2975, 2994 (1984).
[3]J. A. Syage, P. M. Felker, D. H. Semmes, F. Al Adel, and A. H. Zewail, J. Chem. Phys. **82**, 2896 (1985).
[4]P. M. Felker, J. A. Syage, W. R. Lambert, and A. H. Zewail, Chem. Phys. Lett. **92**, 1 (1982); J. A. Syage, P. M. Felker, and A. H. Zewail, J. Chem. Phys. **81**, 2233 (1984).
[5]V. F. Schneider and E. Lippert, Ber. Bunsenges. Phys. Chem. **74**, 624 (1970); **72**, 1155 (1968).
[6]N. Nakashima and D. Phillips, Chem. Phys. Lett. **97**, 337 (1983).
[7]N. Nakashima, M. Masamichi, and N. Mataga, Bull. Chem. Soc. Jpn. **49**, 854 (1976); T. Kobayashi, S. Nagakura, and M. Szwarc, Chem. Phys. **39**, 105 (1979); W. Rettig and M. Zander, Ber. Bunsenges. Phys. Chem. **87**, 1143 (1983).
[8]G. E. Risinger and C. W. Eddy, Chem. Ind. Genie Chim. **1963**, 579; A. Magnus, H. Hartmann, and F. Becker, Z. Phys. Chem. (Leipzig) **197**, 75 (1951); F. Bell and D. H. Waring, J. Chem. Soc. **149**, 267 (1949).
[9]R. Pariser, J. Chem. Phys. **24**, 250 (1956); R. S. Mulliken, *ibid.* **23**, 1997 (1955).
[10]For example, E. B. Wilson, J. C. Decius, and P. C. Cross, in *Molecular Vibrations* (McGraw–Hill, New York, 1955).
[11]A. S. Davydov, in *Theory of Molecular Excitons* (McGraw–Hill, New York, 1962); D. P. Craig and S. H. Walmsley, in *Excitons in Molecular Crystals* (Benjamin, New York, 1968).
[12]The bond lengths were taken from Ref. 5.
[13]G. Zerbi and S. Sandroni, Spectrochim. Acta Part A **24**, 483, 511 (1967).
[14]See for example, J. N. Murrell and J. Tanaka, Mol. Phys. **7**, 363 (1964).
[15]M may be estimated from the oscillator strength f by the relation (Ref. 14) $|M|^2 = 2.15\times 10^{-30}\cdot f/\nu$. ν is the frequency (cm^{-1}) of the absorption maximum and M is in e.s.u. R is assumed the distance between the centers of the two rings. The 9,9′ bond length is 1.5 Å (Ref. 5) and the distance of the center from C9 is the length of a side (1.4 Å). With $f = 0.1$ (Ref. 14), $\nu = 27\,695^2$, $V = -1100$ cm^{-1}.
[16]G. Herzberg, in *Molecular Spectra and Molecular Structure* (Van Nostrand, New York, 1966), Vol. III, p. 119; D. A. Ramsey, Nature **178**, 374 (1956).
[17]In other words, the symmetry of the molecule implies the excited state is a symmetric double well along this coordinate. A wave function of the ground state must be an eigenfunction of the S_1 parity operator, and the even(odd) states in S_0 have zero overlap with odd(even) states of S_1.
[18]A. V. Cunliffe, in *Internal Rotation in Molecules*, edited by W. J. Orville-Thomas (Wiley, New York, 1974), Chap. 7.
[19]The highest order symmetry element of BA is a twofold rotation axis, justifying the choice of a potential with period π.
[20]R. N. Dixon, Trans. Faraday Soc. **60**, 1363 (1964); S. I. Chan and D. Stelman, J. Chem. Phys. **39**, 545 (1963).
[21]L. W. Johnson and R. D. Reiss, in *Numerical Analysis*, 1st ed. (Addison–Wesley, Reading, MA, 1977), p. 330. The matrix solutions were obtained on a VAX 11-780 using the International Mathematics Subroutine Library.
[22]The potential parameters give us the minimum value of $V(\xi)$ and the value of ξ where that occurs. The torsional angle may be obtained by transforming the dimensionless parameter into α. The height is the difference between the height of the perturbation and the minimum value of V.
[23]D. Werst, R. Gentry, and P. Barbara, J. Phys. Chem. **89**, 730 (1985).
[24]K. Yamasaki, K. Arita, O. Kajimoto, and K. Hara (private communication).
[25]H. T. Jonkman and D. A. Wiersma, Chem. Phys. Lett. **97**, 261 (1983); J. Chem. Phys. **81**, 1573 (1984).
[26]J. Murakami, M. Ito, and K. Kaya, J. Chem. Phys. **74**, 6505 (1981).
[27]L. D. Landau and E. M. Lifshitz, in *Quantum Mechanics*, 3rd ed. (Pergamon, Oxford, 1977), p. 136.
[28]S. Fischer, E. W. Schlag, and S. Schneider, Chem. Phys. Lett. **11**, 583 (1971).